

22nd International Conference on

THE PHYSICS OF SEMICONDUCTORS

Volume 1

Vancouver, Canada
August 15 – 19, 1994

Editor

DAVID J. LOCKWOOD
National Research Council of Canada
Institute for Microstructural Sciences
Ottawa, Canada

 **World Scientific**
Singapore • New Jersey • London • Hong Kong

RADIATIVE AND NONRADIATIVE RELAXATION DYNAMICS OF TRANSITION METAL CENTERS IN SEMICONDUCTORS

R. Heitz, L. Podlowski, P. Thurian, A. Hoffmann, and I. Broser
Institut für Festkörperphysik, Technische Universität Berlin, 10623 Berlin, Germany

The results of time-resolved photoluminescence and calorimetric absorption spectroscopy are combined to determine radiative and nonradiative relaxation rates for transition metal centers in semiconductors. Cu^{2+} , Fe^{2+} and Ni^{2+} in various II-VI- and III-V-compounds are investigated as model systems. The oscillator strength of transitions between weakly hybridized states deep in the bandgap is found to be nearly independent of the host lattice whereas transitions involving higher excited states gain oscillator strength from dipole-allowed charge transfer processes. The nonradiative relaxation rate depends on the number of phonons needed to span the transition energy as well as of the electron-phonon interaction. Our results demonstrate unambiguously the importance of both parameters for 3d transition metal centers in semiconductors.

1. Introduction

Transition metals (TM) are well known as optically active defects in semiconductors. Although some prominent centers have been extensively investigated^{1,2} only little information about the competition between radiative and nonradiative relaxation at low temperatures is available to date. The lifetimes τ of excited states showing strong luminescence have been studied using time-resolved luminescence spectroscopy.^{3,4,5} However, no direct access to nonradiative relaxation processes has been given. Recently, calorimetric absorption spectroscopy (CAS) has been introduced as means for the direct detection of nonradiative relaxation processes.⁶ A careful analysis of the CAS results yields the low temperature quantum efficiencies η of the investigated transition.^{7,8,9} The combination of results of time-resolved luminescence and CAS experiments allows for the determination of radiative and nonradiative relaxation rates.

In this paper we present experimental data for Cu^{2+} , Fe^{2+} , and Ni^{2+} in various II-VI- and III-V-semiconductors. Radiative and nonradiative relaxation rates are determined and compared for different centers in order to elucidate general features of the relaxation dynamics of TM centers in semiconductors.

2. Experimental Procedure

For the determination of radiative and nonradiative transition rates we combine data from time-resolved photoluminescence (TRPL) experiments and calorimetric absorption spectroscopy (CAS). CAS detects the increase of sample temperature caused by the generation of phonons during nonradiative relaxation processes. This technique allows an accurate determination of the nonradiative relaxation part, and, thus, the determination of quantum efficiencies η of relaxation processes.⁶ Using time-resolved luminescence spectroscopy we determine the lifetime τ of the excited states, which is limited by radiative as well as nonradiative processes ($\tau^{-1} = W_r + W_{nr}$). The radiative and the nonradiative relaxation rate are given by τ and η :

$$W_r = \frac{\eta}{\tau} \quad \text{and} \quad W_{nr} = \frac{1 - \eta}{\tau} \quad (1)$$

3. Experimental Results

Cu^{2+} introduces two localized 3d-levels within the bandgap of ZnO and ZnS leading to the ${}^2\text{E}-{}^2\text{T}_2$ absorption and emission in the near IR spectral region.^{10,11} Here, we determine the low temperature quantum efficiency η of the ${}^2\text{E}-{}^2\text{T}_2$ luminescence to be $(29 \pm 4) \%$ and $(54 \pm 4) \%$ as well as luminescence decay times τ of 200 ns and 350 ns for ZnO and ZnS, respectively. Thus, W_r amounts to 1.5 MHz in both systems within the experimental error, whereas W_{nr} differs significantly with 3.6 MHz (ZnO) and 1.3 MHz (ZnS).

The internal $\text{Fe}^{2+}({}^5\text{T}_2-{}^5\text{E})$ relaxation in GaAs, GaP, and InP leads to an intense luminescence band around 0.4 eV.¹ However, the CAS experiments show a considerable contribution of nonradiative processes. The low temperature quantum efficiencies η are well below 1 with $(26 \pm 4) \%$ in GaP, $(35 \pm 5) \%$ in GaAs and $(47 \pm 6) \%$ in InP. Though the observed luminescence decay times τ show a similar variation,¹²⁻¹⁴ the radiative transition rates W_r are found to be equal within experimental error. The different relaxation dynamics of Fe^{2+} in III-V compounds result from an enhanced nonradiative relaxation probability for GaP and GaAs compared to InP.

Ni^{2+} is a multilevel defect in the widegap II-VI compounds giving rise for a variety of radiative and nonradiative relaxation channels. However, analog to the Cu^{2+} and Fe^{2+} transitions the lowest energy ${}^3\text{T}_1(\text{F})-{}^3\text{T}_2(\text{F})$ transition can be discussed in a two-level system. This transition leads to strong absorption bands,² whereas the inverse emission bands are often faint and difficult to observe. Luminescence decay times τ between $0.35 \mu\text{s}$ (ZnS) and $70 \mu\text{s}$ (ZnSe) are reported,³ indicating a pronounced host dependence of the relaxation processes. The CAS experiments demonstrate a similar spreading of the low temperature quantum efficiency η varying between $(0 \pm 4) \%$ in ZnO and $(47 \pm 3) \%$ in ZnSe. The low quantum efficiency of only 3 % in ZnS makes it impossible to determine a reliable radiative transition rate in view of the larger experimental error.

At higher energies the spin- and symmetry-allowed ${}^3\text{T}_1(\text{F})-{}^3\text{T}_1(\text{P})$ transition leads to

Table 1. Experimental low temperature luminescence decay times τ and quantum efficiencies η (accuracy is about 4 %) of intracenter transitions of TM's and the resulting radiative W_r and nonradiative W_{nr} transition rates.

transition	host	τ	η (%)	W_r (Hz)	W_{nr} (Hz)
Cu^{2+} (${}^2\text{E}-{}^2\text{T}_2$)	ZnO	350 ns	29	$1.5 \cdot 10^6$	$3.6 \cdot 10^6$
	ZnS	200 ns	54	$1.5 \cdot 10^6$	$1.3 \cdot 10^6$
Fe^{2+} (${}^5\text{T}_2-{}^5\text{E}$)	GaAs	$8.5 \mu\text{s}^{14}$	35	$4.1 \cdot 10^4$	$7.7 \cdot 10^4$
	GaP	$6.6 \mu\text{s}^{13}$	26	$3.9 \cdot 10^4$	$11.4 \cdot 10^4$
	InP	$11 \mu\text{s}^{12}$	47	$4.3 \cdot 10^4$	$5.7 \cdot 10^4$
Ni^{2+} (${}^3\text{T}_2(\text{F})-{}^3\text{T}_1(\text{F})$)	ZnO	-	0	-	-
	ZnS	$0.35 \mu\text{s}^3$	3	$10^4 - 10^5$	$2.8 \cdot 10^6$
	ZnSe	$70 \mu\text{s}^3$	47	$6.7 \cdot 10^3$	$7.7 \cdot 10^3$
	CdS	-	5	-	-
Ni^{2+} (${}^3\text{T}_1(\text{P})-{}^3\text{T}_1(\text{F})$)	ZnO	-	0	-	-
	ZnS	100 ps	14	$1.4 \cdot 10^9$	$8.6 \cdot 10^9$
	ZnSe	100 ps	7	$0.7 \cdot 10^9$	$9.3 \cdot 10^9$
	CdS	400 ps	16	$0.4 \cdot 10^9$	$2.1 \cdot 10^9$

prominent near IR absorption and emission. We observe extraordinary short luminescence decay times τ of only some hundred ps. Although the CAS experiments prove predominant nonradiative relaxation of the $^3T_1(P)$ excited state, the determined quantum efficiencies η around 10 % still indicate strongly enhanced radiative transition rates up to the 10^9 Hz range.

Table 1 summarizes the experimentally determined lifetimes τ and quantum efficiencies η and gives the resulting radiative (W_r) and nonradiative (W_{nr}) transition rates.

4. Discussion

The crystal field transitions of TM's are on principle dipole-forbidden due to their d-d character. The observed transition rates indicate a break-down of Laporte's rule due to the admixture of p-type wave functions by the covalent bonding (p-type valence band states) and configuration mixing (4p-state of the TM) enabled by the lack of inversion symmetry. The experimental results (Tab. 1) show that W_r is nearly host independent for the infrared transitions between states deep in the bandgap. This indicates that configuration mixing gives the dominating contribution to the oscillator strength. For the II-VI compounds calculations¹⁵ support this interpretation. However, for Fe^{2+} in the more covalent III-V compounds a large contribution of valence band states is expected, too. On the contrary, the large increase of W_r in case of the $Ni^{2+}(^3T_1(F)-^3T_1(P))$ transition shows that the oscillator strength is borrowed from the dipole-allowed acceptor-type charge transfer transition.⁵

Table 1 demonstrates that for all investigated transitions nonradiative multiphonon processes are important even at liquid He temperatures. Due to the low excitation densities employed and the semi-insulating character of the investigated samples Auger-type processes can be excluded. The probability of multiphonon transitions depends basically on the number of phonons N needed to span the transition energy and on the electron-phonon coupling strength. TM's in semiconductors are subject to an intermediate electron-phonon interaction making theoretical predictions difficult.

Without electron-phonon coupling an exponential decrease of the multiphonon transition probability W_{nr} with increasing N is expected and has been verified for 4f centers.¹⁶ For 3d-

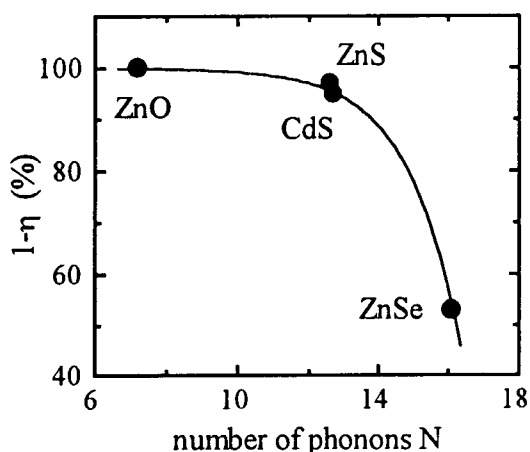


Figure 1. The nonradiative relaxation part $1 - \eta$ versus the number of phonons N for the $Ni^{2+}(^3T_2(F)-^3T_1(F))$ transition.

elements the electron-phonon interaction has to be taken into account, but still a systematic correlation between W_{nr} and N can be stated. For the $Cu^{2+}(^2E-^2T_2)$ transition W_{nr} is much higher in ZnO than in ZnS, which corresponds to the fact that the multiphonon transition involves 10 phonons in ZnO instead of 16 in ZnS. The lifetime τ of the $Ni^{2+}(^3T_2(F))$ state is known only for ZnS and ZnSe. However, as discussed above it is reasonable to assume a similar radiative transition rate W_r of about 10^4 Hz. Fig.1 shows the nonradiative relaxation part $1 - \eta$ versus the number of phonons N

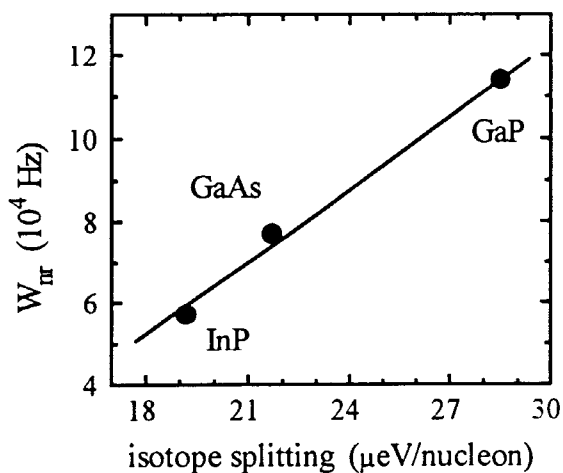


Figure 2. The nonradiative transition rate W_{nr} versus the isotope splitting for the $Fe^{2+} (^5T_2-^5E)$ transition. The isotope shift is a measure for the electron-phonon coupling strength.

magnitude is a measure for the coupling strength.¹⁷ Fig. 2 shows clearly the correlation between W_{nr} and the isotope splitting demonstrating that even a weak dynamical Jahn-Teller effect can drastically increase the multiphonon relaxation probability.

5. Conclusion

The present paper demonstrates that the combination of TRPL and CAS gives detailed insight into the low temperature relaxation processes. The radiative transition rates between states deep in the bandgap are found to be nearly independent of the host compound. The variation of the luminescence decay times is caused by the nonradiative processes. For TM's in semiconductors the significance of both the number of phonons needed to span the transition energy and the electron-phonon coupling is proved.

¹ S.G. Bishop, in *Deep Centers in Semiconductors*, ed. S. Pantilides (Gordon&Breach, New York, 1986), p. 541.

² H.A. Weakliem, *J. Chem. Phys.* **36**, 2117 (1962).

³ G. Goetz and H.-J. Schulz, *J. Lumin.* **40/41**, 415 (1988).

⁴ G. Guillot, C. Benjeddou, P. Leyral, and A. Nouailhat, *J. Lumin.* **31&32**, 439 (1984).

⁵ R. Heitz, A. Hoffmann, and I. Broser, *J. Lumin.* **53**, 359 (1992).

⁶ L. Podlowski, A. Hoffmann, and I. Broser, *J. Cryst. Growth* **117**, 698 (1992).

⁷ R. Heitz, A. Hoffmann, and I. Broser, *Optical Materials* **1**, 75 (1992).

⁸ L. Podlowski, R. Heitz, P. Thurian, A. Hoffmann, and I. Broser, *J. Lumin.* **58**, 252 (1994).

⁹ I. Broser, L. Podlowski, P. Thurian, R. Heitz, and A. Hoffmann, *J. Lumin.* **60&61**, 588 (1994).

¹⁰ R.E. Dietz, H. Kamimura, M.D. Sturge, and A. Yasir, *Phys. Rev.* **132**, 1559 (1963).

¹¹ I. Broser, H. Maier, and H.-J. Schulz, *Phys. Rev.* **140**, 2135 (1965).

¹² P.B. Klein, J.E. Fournaux, and R.L. Henry, *Phys. Rev.* **B29**, 1947 (1984).

¹³ P.B. Klein and K. Weiser, *Solid State Commun.* **41**, 365 (1982).

¹⁴ K. Pressel, G. Bohnert, G. Rückert, A. Dörnen, and K. Thonke, *J. Appl. Phys.* **71**, 5703 (1992).

¹⁵ V. Gomathy, C. Basu, and U.S. Ghosh, *phys. stat. sol. (b)* **86**, 379 (1978).

¹⁶ M.J. Weber, *Phys. Rev.* **B8**, 54 (1973).

¹⁷ R. Heitz, L. Podlowski, A. Hoffmann, and I. Broser, Proc. 8th SIMS, Warschau (1994), in press..

confirming the expected behavior.

An intermediate electron-phonon coupling is expected to enhance the multiphonon emission rate W_{nr} . Due to the still present influence of N for most systems it is difficult to separate the effect of the electron-phonon coupling. Nevertheless, the $Fe^{2+} (^5T_2-^5E)$ transition energy corresponds to about 10 phonons in all investigated III-V compounds making the electron-phonon coupling the crucial parameter. In principle, the evaluation of the electron-phonon coupling strength needs sufficient fine structure data and detailed calculations. However, isotope shifts observed for the internal Fe^{2+} transition indicate a dynamical coupling to local T_2 modes in the excited 5T_2 state and their